Intrinsic feedback and bistable switching in Y-branched nanojunctions

S. Reitzenstein, L. Worschech, D. Hartmann, and A. Forchel
Technische Physik and Wilhelm Conrad Röntgen Research Center for Complex Material Systems, Universität Würzburg, Am Hubland, D-97074 Würzburg, Germany

(Received 8 January 2010; revised manuscript received 6 March 2010; published 23 April 2010)

We present intrinsic feedback and nonlinear switching in Y-branched nanotransistors. For this type of mesoscopic transistor the gate efficiency depends on the density of states in the gate electrode which is altered by voltage shifts at the drain. This nonclassical property of a Y junction introduces positive voltage feedback which leads to pronounced nonlinearities and is exploited to demonstrate highly efficient gating and bistable switching. Our results demonstrate that the efficiency of nanoscaled transistors can be enhanced dramatically by exploiting quantum effects.

DOI: 10.1103/PhysRevB.81.153411 PACS number(s): 68.65.−k, 72.20.Ht, 73.23.−b

Nonlinear transport characteristics of mesoscopic conductors have attracted enormous scientific interest in recent years. For instance, unidirectional current flow has been studied in two-terminal tunneling ratchets[1] and self-switching devices.[2] Of particular interest are three-terminal junctions which show a large variety of nonlinear transport phenomena. The most prominent example is the ballistic rectification effect[3] which has been observed in Y-branched nanojunctions up to room temperature[4] and has initiated intensive theoretical studies.[5–7] Moreover, if combined with side gates the Y-branched nanojunctions allow for gain[8,9] and even bistable switching in the presence of external voltage feedback.[10]

Switching in Y-branched nanojunctions is enhanced by a self-gating effect[8,11] which is not expected in macroscopic conductors. This leads to an important issue in mesoscopic physics; namely, the gating of charged carriers in nanoscaled conductors. While the transport in conventional transistors is controlled very precisely by external gate voltages, classically unexpected features can occur in mesoscopic pendants and the quantum capacitance needs to be considered.[12] In fact, the capacitance of mesoscopic conductors depends on the density of states (DOS) of the "mesoscopic capacitor plates" as well as on the reflection probability between the plates when a leaky system is considered.[13] Taking into account a local partial density of states this semiclassical result has been extended to describe not only the linear but also the second-order nonlinear capacitance of leaky nanocapacitors[14,15] which are characterized by a voltage-dependent capacitance.[16] Hence, it is clear that the capacitance of mesoscopic conductors, and as a result also the current flow in these structures, depend sensitively on the particular bias condition and nonlinear effects as well as bistabilities are expected to occur.

In this Brief Report we investigate the role of quantum capacitance on the nonlinear transport in Y-branched nanojunctions. We have chosen three terminal junctions because they represent a very attractive model system to control the current flow between two terminals via the voltage applied to the third terminal acting as gate. Moreover, this system provides an internal feedback coupling mediated by the capacitive coupling between the branches of the Y junction.[8] The internal feedback coupling allows for the observation of pronounced nonlinear transport phenomena such as a resonancelike transfer characteristic at the transition from capacitive gating to a space-charge enhanced control of the source current. The underlying concept could be the basis for an advanced transistor concept which utilizes the influence of the output voltage on the DOS in the gate electrode to dynamically increase the gate efficiency. We show that for an asymmetric Y junction the internal feedback mechanism results even in bistable switching.

The Y junctions are based on a modulation-doped GaAs/AlGaAs heterostructure with a high mobility two-dimensional electron gas (2DEG) located 80 nm below the surface. The 2DEG is characterized by a mobility $\mu=0.8\times10^6$ cm^2/Vs and a electron density of $n=3.6\times10^{11}$ cm^{-2} determined at $T=4.2$ K. High-resolution electron-beam lithography and chemical etching were used to realize the Y junctions. Figure 1(b) shows a scanning electron microcopy (SEM) image of a Y junction which is separated by 90-nm-deep etched trenches from the left and the right side gates. The transport measurements were performed at $T=4.2$ K. As sketched in Fig. 1(b) bias voltages $V_{bias,l}$ and $V_{bias,r}$ were applied in series with resistors $R_{bl}=10$ MΩ and $R_{br}=100$ kΩ to the left and right branch, respectively, with the stem of the Y junction connected via a resistor $R_s=12$ kΩ to ground. Voltages V_{gl} and V_{gr} applied to the left and right side gates were used to tune the Y junction asymmetrically into a regime were the right branch is not conductive for $V_{bias,r}>0$ while finite conductance was measured for the left branch. Gating of the device section connecting the stem with the left branch was investigated by detecting the voltages V_{bl} (output signal) and V_{br} at the left and right branch as a function of the bias voltage $V_{bias,r}$ (input signal) with $V_{bias,l}$ acting as parameter. The current in the stem (I_s), left branch (I_l), and right branch (I_r) was determined by the voltage drop along the respective external resistor.

Figure 1(a) shows the transfer characteristic of a symmetric Y junction for several bias voltages $V_{bias,l}$ ranging from 0 to 1.8 V. For $V_{bias,l}=0$ the voltage at the left branch equals to zero when positive voltages are applied to the right branch ($V_{bias,r}>0$) while it becomes negative for $V_{bias,r}$ falling below −100 mV, i.e., rectification of the input voltage is observed. Such a rectification behavior has been predicted and observed for three terminal ballistic junctions.[5,17] The decrease in the output voltage V_{bl} with decreasing input voltage $V_{bias,r}<-100$ mV is associated with the inset of electron flow from the right branch into the branching section. For $V_{bias,l}=0.2$ V the output signal is shifted to more positive

 ©2010 The American Physical Society

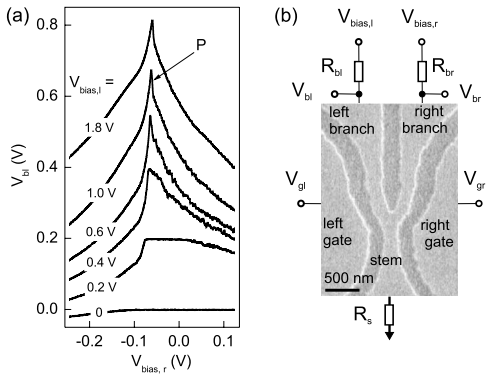

FIG. 1. (a) Transfer characteristics of a symmetric Y junction. (b) SEM image of a symmetric Y junction and a schematic view of the measurement setup.

values with V_{bl}=0.2 V, i.e., I_l=0, in the voltage range -70 mV$<V_{bias,r}<10$ mV. The decrease in the output voltage V_{bl} for $V_{bias,r}<-70$ mV is again attributed to the injection of electrons from the right-branch section. Input voltages $V_{bias,r}>10$ mV lead to an inverterlike behavior due to a capacitive coupling between the right branch and the branching section. Interestingly, the input voltage range associated with I_l=0 becomes smaller with increasing $V_{bias,l}$ and diminishes completely for $V_{bias,l}>0.4$ V. In fact, a pronounced voltage peak evolves in the $V_{bl}(V_{bias,r})$ characteristic at $V_{bias,r}=V_p$ where the regimes controlled by the capacitive gating and the injection of electrons, respectively, merge. An important aspect of the strong nonlinear transfer characteristic is the input voltage dependent slope $\eta_g=dV_{bl}/dV_{bias,r}$ in the capacitively controlled gating regime: η_g at first increases slightly with decreasing $V_{bias,r}$ before a strong increase sets in close to V_p [labeled P in Fig. 1(a)].

It is important to note, that the input voltage for which injection sets in, i.e., V_p, depends on the maximum output voltage, $V_{bl,max}$, of the respective input-output trace. In fact, V_p increases with $V_{bl,max}$ in a parabolic way which is depicted in Fig. 2(a) where V_p is plotted as a function of $V_{bl,max}$ for different $V_{bias,l}$. The dependence of V_p on $V_{bl,max}$ can be

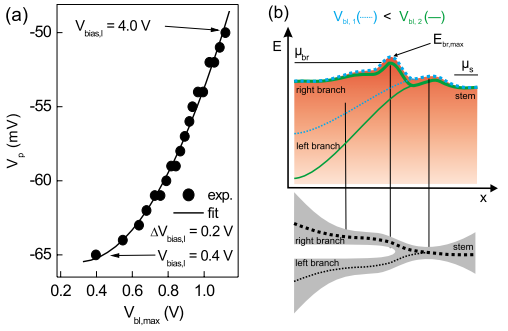

FIG. 2. (Color online) (a) Voltage V_p at which the maximum ($V_{bl,max}$) in the $V_{bl}(V_{bias,r})$ trace occurs as a function of $V_{bl,max}$. (b) Qualitative illustration of the electrostatic potential along the right branch-stem (thick lines) and left branch-stem (thin lines) sections of the Y junction for two voltages, $V_{bl,1}$, $V_{bl,2}$ with $V_{bl,1}<V_{bl,2}$, applied to the left branch. An increase in V_{bl} leads to a reduction in $E_{br,max}$ which in turn lowers V_p.

approximated in the relevant voltage interval by

$$V_p(V_{bl}) = V_{p0} + \alpha V_{bl} + \beta V_{bl}^2 \quad (1)$$

with the fitting parameters $V_{p0}=-63$ mV, $\alpha=-1.4\times10^{-2}$, and $\beta=2.4\times10^{-2}$ V^{-1}. The voltage V_p is associated with the onset of electron flow from the right branch into the branching section when the chemical potential μ_{br} in the respective reservoir equals the maximum $E_{br,max}$ of the conduction band along this section. Thus, our observation indicates that the output voltage at the left branch influences the potential along the right branch. In order to illustrate this interpretation qualitatively, we plotted the electrostatic potential along the device section between the branches and the stem of the Y junction in Fig. 2(b) for two voltages, V_{bl}, applied to the left branch. The potential $E_{br,max}$ which determines the threshold for current injection is influenced by V_{bl} due to the coupling of the branches. In particular, $E_{br,max}$, and as a consequence V_p, decrease when V_{bl} becomes more positive.

The input voltage-dependent slope η_g of the transfer characteristic in the gating regime in combination with the influence of the output voltage on the barrier along the right branch result in an internal feedback mechanism which significantly affects the switching properties of nanoscaled Y junctions. In order to explain this feedback mechanism we consider that the electrochemical capacitance C of a nanoscaled leaky capacitor depends on the density of states, dN_1/dE and dN_2/dE, of the mesoscopic capacitor plates as well as on the reflection probability R between the plates

$$C = R/(C_0^{-1} + D_1^{-1} + D_2^{-1}) \quad (2)$$

with the geometrically defined electrostatic capacitance C_0 and the quantum capacitance $D_i=e^2dN_i/dE$ of the capacitor plate i.[13] According to Eq. (2), C depends for a given C_0 and R on the density of states in the capacitor plates. By adopting this concept to the Y junction, it is possible to describe the voltage dependent slope η_g. Here the slope η_g is a measure of the gating efficiency which in turn depends on the electrochemical capacitance C_g between the right branch and the branching section. Thus, in the present configuration a reduction in the gate voltage results in a higher electrochemical potential, and DOS, in the right branch which enhances the gating efficiency. As a result, the slope of the input-output trace rises when $V_{bias,r}$ approaches V_p. So far, only a shift of the chemical potential in the right branch due to a change in the gate voltage has been considered. However, an increase in V_{bl} is associated with a lowering of the conduction band along the right branch [Fig. 2(b)]. As a result the DOS (as well as η_g) increases for $V_{bias,r}$=const.. This is an important feature since it means that the capacitive coupling between the gate and the channel is influenced by the output signal at the drain (V_{bl}) which introduces a positive internal feedback mechanism. We will show below that the internal feedback can lead to bistable switching in an asymmetric Y junction. For a symmetric Y junction, both the DOS in the gating branch and the reflectivity R between the gate and the channel have an effect on the switching characteristics according to Eq. (2). In fact, gate leakage which is associated with $R<1$ leads to a breakdown of the feedback circle.

Phenomenologically, the $V_{bl}(V_{bias,r})$ dependence can be

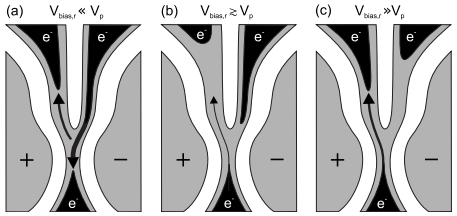

FIG. 3. Diagrams illustrating schematically the electrical characteristics of a symmetrical Y junction for three different values of V_{br}: (a) injection regime, (b) gating regime near the transition to the injection regime, and (c) gating regime. Black arrows illustrate the motion of electrons with their width being a measure of the magnitude of the attributed current.

described by a model based on the schematic illustrations given in Fig. 3 for three bias voltage configurations. Black areas indicate the penetration of electrons from the 2D reservoirs into individual sections of the Y branch, where the penetration depth depends on the chemical potential of the electrons in the particular reservoir. Panel (a) of Fig. 3 corresponds to a bias regime associated with $V_{bias,r} \ll V_p$. Due to the negative potential applied to the right-branch reservoir hot electrons are injected into the Y branch and traverse the branching section in a quasiballistic way before they drain off into the stem. Only a small portion of the injected electrons are attracted by the positive bias voltage into the left branch. The transition from the injection regime into the gating regime changes the electrical characteristics substantially and results in a situation illustrated in Fig. 3(b) for $V_{bias,r} \gtrsim V_p$ [see also Fig. 2(b)]. The right branch is electrically isolated from the Y junction since the barrier height $E_{br,max}$ exceeds the chemical potential of the respective reservoir. In addition, the transition from injection to gating leads to a change of sign in I_s to match that of I_l for $V_{bias,r} > V_p$. In the gating regime [Fig. 3(c), $V_{bias,r} \gg V_p$] the conductance G_{sl} between the stem and the left branch is controlled capacitively by the voltage applied to the right branch. The corresponding gating efficiency η_{br} increases strongly when electrons penetrate from the reservoir into the right branch section. For the case of $V_{bias,r} \gg V_p$ the right branch is depleted and gating is due to the long-range Coulomb interaction between the electrons in the right-branch reservoir and carriers in the branching section. With decreasing V_{br}, electrons start to significantly penetrate into the right branch which reduces the distance between the gating electrons and the branching section. This penetration of electrons and the associated space-charge effect lowers significantly the current flow into the left branch due to a short-range Coulomb interaction.

Taking the bias voltage-dependent penetration of electrons into account we introduce a model which relates the strong increase in V_{bl} for $V_{bias,r} \gtrsim V_p$ to a dramatic enhancement of η_{br} and the capacitance C_{br} between the right-branch reservoir and the Y junction, respectively. In the gating regime with negligible current I_r we neglect the voltage drop at R_{br} and set $V_{br}=V_{bias,r}$. The voltage at the left branch is then related to I_l by

$$V_{bl} = V_{bias,l} - R_{bl} I_l = V_{bias,l} - R_{bl} G_{sl} (V_{bl} - V_{st}), \qquad (3)$$

where V_{st} denotes the voltage at the stem reservoir. G_{sl} in turn depends on the voltage at the right branch and can be expressed using a switching parameter γ (Ref. 8)

$$G_{sl} = (1/2)(1-\gamma) = (1/2) G \{1 + \tanh[\eta_{br}(V_{br} - V_{th})/V_s + c_{wp}/V_s]\} \qquad (4)$$

with G, the maximum conductance between the stem and the left branch, and the switching parameter, V_s.[11] The constant c_{wp} considers the influence of the side gates on the working point of the Y junction and V_{th} denotes the threshold voltage above (below) which V_{br} enhances (reduces) the conductance defined initially by the side gates. As sketched in Fig. 3 the penetration of electrons into the right branch changes with V_{br} which is supposed to influence C_{br}.[14] Therefore, the switching efficiency $\eta_{br} \propto C_{br}$ increases strongly for $V_{br} \rightarrow V_p$. In a phenomenological approach we express the corresponding efficiency η_{br} by

$$\eta_{br} = \eta_{sr} + \eta_{lr} = \eta^*_{sr}/[V_{br} - V_p(V_{bl})] + \eta_{lr}, \qquad (5)$$

where η_{sr} (η_{lr}) considers the short-range (long-range) Coulomb interaction. We solved these equations numerically with $V_{st} \approx 0$ and calculated V_{bl} as a function of V_{br}. The calculated values are plotted in Fig. 4(a) for three values of η^*_{sr}/V_s. Neglecting the short range coupling ($\eta^*_{sr}/V_s=0$, dotted line) the very steep flank observed experimentally in the proximity of V_p is absent. In contrast, the slope of the traces associated with $\eta^*_{sr}/V_s > 0$ increases strongly for V_{br} approaching V_p. The best agreement with the experimental data was found for $G=4.0\times10^{-7}\ \Omega^{-1}$, $\eta^*_{sr}/V_s=4.5\times10^{-2}$, $\eta_{lr}/V_s=6.1\ \mathrm{V}^{-1}$, $V_{th}=56.1$ mV, $c_{wp}/V_s=-1.0$.

An interesting feature of Eq. (5) is the dependence of η_{sr} on V_{bl} through Eq. (1) which introduces the positive intrinsic feedback in the gating regime. In order to understand this feedback mechanism one has to consider that the input voltage V_{br} controls the output signal V_{bl} with a gating efficiency η^*_{sr} depending on $V_{br}-V_p$. The backcoupling of V_{bl} lowers V_p (Fig. 2) and, as a consequence, V_{bl} changes in a strongly nonlinear way when V_{br} is varied. We predict that intrinsic feedback leads to bistable switching in case the condition $dV_{bl}/dV_{br} \times dV_p/dV_{bl} \lesssim -1$ is satisfied. It is useful to compare the above theoretical considerations with the experimental data. From Fig. 4(a), I_r/I_l and V_{bl} are plotted versus $V_{bias,r}$ we extracted a maximum voltage gain of $(dV_{bl}/dV_{br})_{max}=-50$ at $V_{bl} \approx 0.7$ V. Furthermore it is possible to calculate the intrinsic feedback parameter $dV_p/dV_{bl}|_{V_{bl}=0.7\ \mathrm{V}}=0.020$ using Eq. (1), i.e., $[(dV_{bl}/dV_{br})|_{V_{bl}=0.7\ \mathrm{V}} \times (dV_p/dV_{bl})_{max}]=-1$ which should lead to bistable switching. However, bistable switching is absent for the symmetric Y junction since the syncopate between the right branch and branching section becomes leaky for $V_{br} < V_p$. This limits not only C_{br} and the gating efficiency, η_{sr}, but also the maximum achievable voltage gain dV_{bl}/dV_{br}, respectively.[13]

In order to observe bistable switching, we realized an asymmetric Y junction with a small constriction close the branching section [cf. Fig. 5 (inset)]. This Y junction is characterized by an extraordinarily good transfer characteristic and shows a differential voltage gain of up to −580 as depicted in Fig. 4(b) for $V_{bias,l}=1.6$ V. In addition, the ratio I_r/I_l representing a measure of the gate leakage is strongly

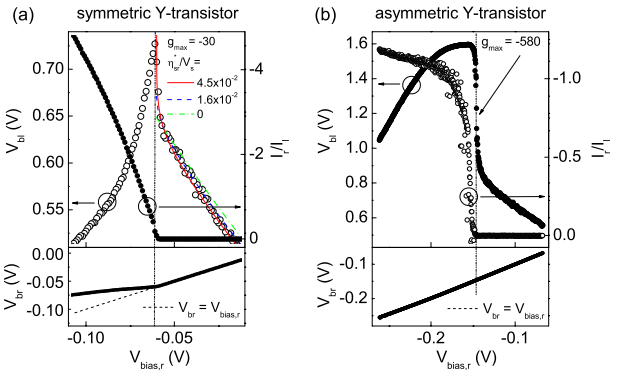

FIG. 4. (Color online) (a) Transfer characteristics of a symmetric and (b) an asymmetric Y junction, respectively. The dashed vertical lines indicate the input voltage for which the transition from the gating regime to the injection regime occurs. An absence of gate leakage currents would mean $V_{br}=V_{bias,r}$ which is indicated by the dashed lines in the lower panels. (a) The $V_{bl}(V_{bias,r})$ trace of the symmetric Y junction shows a pronounced nonlinearity associated with a maximum voltage gain of −30. The onset of leakage current is reflected in the increase in ratio I_r/I_l and the deviation between V_{br} and $V_{bias,r}$. Calculated values according to Eqs. (3)–(5) are plotted for three values of the internal switching efficiency η^*/V_s. Best agreement between experiment and theory is obtained for $\eta^*/V_s=4.5\times10^{-2}$. (b) The input-output characteristic of the asymmetric Y junctions exhibits a significantly higher voltage gain $g_{max}=-580$. Due to the constriction close to the branching section and the associated tunnel barrier (cf. Fig. 5, inset), the leakage current from the right branch into the branching section is significantly reduced which is reflected in a lower I_r/I_l ratio and $V_{br}\approx V_{bias,r}$.

reduced. This is also reflected in the $V_{br}(V_{bias,r})$ trace deviating only slightly from the ideal $V_{br}=V_{bias,r}$ line in the lower panel of Fig. 4(b). Furthermore, leakage currents set in not before the gate voltage falls below the regime of maximum differential gain so that the asymmetric Y junction should show a bistable switching behavior. In fact, the input-output trace shown in Fig. 5 demonstrates that bistable operation of the Y junction is possible without any external feedback coupling. The data was obtained at 4.2 K for $V_{bias,l}=2.5$ V and a voltage sweep rate of 25 μeV/s. The depicted transfer characteristic clearly reflects the bistable behavior of the asymmetric Y junction by the abrupt switching from one stable state to the other associated with a pronounced hysteresis of 2 meV between the up and down sweeps. The present bistable switching behavior needs to be distinguished from bistable switching observed for a Y junction in the presence of an additional *external* feedback.[10] In contrast to this type of bistable switching which requires an external connection between one side gate and the opposing branch of the Y junction, the present approach relies only on the internal feedback mechanism which is very advantageous in light of device integration. However, the strength of the internal feedback is somewhat lower which explains the smaller switching hysteresis of 2 meV if compared to 135 meV reported for an externally coupled Y junction under similar bias conditions.[10] With respect to possible memory applications it is interesting to note that the bistability in the asymmetric Y junction is stable over several hours and remains up to temperatures of about 20 K when a transition from bistable switching to amplification of the input voltage occurs. A better temperature performance might be obtained by reducing the width of the constriction close to the branching section and by enhancing the internal feedback coupling due to an improved device design.

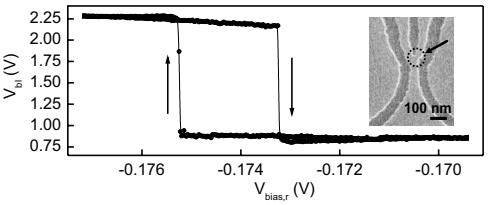

FIG. 5. Bistable switching of an asymmetric Y junction. The V_{bl} vs $V_{bias,r}$ characteristic shows a clear bistable switching behavior associated with an hysteresis of 2 mV between the up and down sweep. Inset: SEM image of an asymmetric Y junction.

In summary, we have demonstrated an intrinsic feedback mechanism which allows one to tune a Y-branched nanojunction from a linear-response regime into a strongly nonlinear regime associated with a pronounced bistable switching. Our observation gives a distinct insight in the gating properties of ultrasmall junctions and explores a gating mechanism based on the quantum capacitance of nanoscaled conductors which has high potential for future transistor concepts.

This work was supported by the European Commission through the IST Programme Project SUBTLE and the state of Bavaria. Expert technological assistance by M. Emmerling and S. Kuhn is gratefully acknowledged.

[1] H. Linke *et al.*, Science **286**, 2314 (1999).
[2] A. M. Song *et al.*, Appl. Phys. Lett. **83**, 1881 (2003).
[3] L. Worschech *et al.*, Appl. Phys. Lett. **79**, 3287 (2001).
[4] D. Wallin *et al.*, Appl. Phys. Lett. **89**, 092124 (2006).
[5] H. Q. Xu, Appl. Phys. Lett. **80**, 853 (2002).
[6] D. Csontos and H. Q. Xu, Phys. Rev. B **67**, 235322 (2003).
[7] A. N. Jordan and M. Büttiker, Phys. Rev. B **77**, 075334 (2008).
[8] S. Reitzenstein *et al.*, Phys. Rev. Lett. **89**, 226804 (2002).
[9] D. Hartmann *et al.*, Phys. Rev. B **75**, 121302 (2007).
[10] S. Reitzenstein *et al.*, Appl. Phys. Lett. **82**, 1980 (2003).
[11] Jan-Olof J. Wesström, Phys. Rev. Lett. **82**, 2564 (1999).
[12] S. Luryi, Appl. Phys. Lett. **52**, 501 (1988).
[13] T. Christen, and M. Büttiker, Phys. Rev. Lett. **77**, 143 (1996).
[14] X. Zhao *et al.*, Phys. Rev. B **60**, 16730 (1999).
[15] J. G. Hou *et al.*, Phys. Rev. Lett. **86**, 5321 (2001).
[16] B. Wang *et al.*, Appl. Phys. Lett. **74**, 2887 (1999).
[17] I. Shorubalko *et al.*, Appl. Phys. Lett. **83**, 2369 (2003).